

The load dependence of hardness in alumina–silver composites

A.K. Dutta ^a, N. Narasaiah ^b, A.B. Chattopadhyaya ^c, K.K. Ray ^{b,*}

^aDepartment of Mechanical Engineering, Bengal Engineering College (Deemed University), Howrah 711103, India

^bDepartment of Metallurgical and Materials Engineering, Indian Institute of Technology, Kharagpur 721302, India

^cDepartment of Mechanical Engineering, Indian Institute of Technology, Kharagpur 721302, India

Received 5 June 2000; received in revised form 16 June 2000; accepted 22 August 2000

Abstract

The room temperature Knoop micro-hardness properties of three alumina–silver composites vis-a-vis a monolithic alumina have been investigated at different indentation loads. The composites have been developed using conventional pressureless sintering at 1550°C and these consisted of 1.6, 3.38 and 5.01% by volume of silver particles. It has been shown that the measured Knoop hardness values of these materials sensitively depend on the applied load of indentation. But following an emerging analytical technique, the composites can be assigned some unique true hardness values, which are functions of their silver content. © 2001 Elsevier Science Ltd and Techna S.r.l. All rights reserved.

Keywords: B. Composites; C. Hardness; D. Al_2O_3

1. Introduction

In recent years a variety of metal particle reinforced alumina matrix composites (AMC) are being developed to examine their potential for structural applications. This new class of materials retain several key advantages of monolithic alumina like low density, chemical inertness, and good oxidation resistance with the additional merit of enhanced toughness though often at the cost of minor degradation of hardness. Several variations of such AMCs are found reported in the literature with additions of different metals like Al [1,2], Ni [3–5], Fe [6], Mo [7,8], Ag [9–12] etc. The mechanical properties of significant interest for these materials are hardness, strength, fracture toughness, creep resistance and thermal shock resistance. This report focuses on the characterization of intrinsic hardness values of these materials.

The measurement of hardness of brittle materials is usually carried out with the help of Vickers or Knoop indentation at various loads. Several recent reports like the ones by Li et al. [13], Ray and Dutta [14], Quinn and Quinn [15], Li and Bradt [16] have shown that the

magnitudes of indentation load have profound influence on the evaluated hardness value of ceramic and glasses. This phenomenon is often referred as indentation size effect. As a consequence, it becomes difficult to make comparative assessment of the hardness property of the reported metal particle toughened AMCs if such estimates do not correspond to identical indentation loads. This is apart from the fact that such hardness values are also influenced by the nature of the processed materials particularly with respect to their relative densities or microstructures. The ambiguity associated with a hardness measurement gets extended in the estimation of indentation fracture toughness (IFT) of these materials too, because most of the existing formulae to estimate IFT of AMCs incorporate the magnitude of hardness of the material [14].

The mechanical properties of metal particle reinforced AMCs are known to be sensitively dependent on the nature of the interface formed between the metal particle and the matrix. The formation of spinels at such interfaces of these composites degrades their mechanical properties. This aspect has been carefully taken into account while preparing such composites by the use of controlled environments [3–8]. It is known from the existing literature that a relatively cleaner interface can be achieved only in the case of alumina–silver composites by the simple pressureless sintering. The earlier

* Corresponding author. Tel.: +91-3222-55221; fax: +91-3222-55303.

E-mail address: kkrmt@metal.iitkgp.ernet.in (K.K. Ray).

reports of Wang et al. [9] and Chou and Tuan [11] have provided distinct experimental evidences for this fact. Thus alumina–silver composites can be considered as an ideal system for examining the load-dependence of hardness in metal particle reinforced AMC systems. In the earlier investigations [9,11], the hardness measurements are found reported with the use of Vickers indentation only at some fixed load values. An examination of such hardness values of these systems estimated at a fixed load of indentation provides only an apparent relative comparison of this property. The uncertainty related to the estimation of absolute magnitudes of intrinsic hardness does not permit one to make a true grading of these materials with respect to this property.

The objectives of this study are (i) to develop a series of alumina–silver composites with different volume fractions of silver, (ii) to examine their microstructural characteristics and (iii) to determine their intrinsic hardness values by carrying out a series of measurements at different loads with subsequent analysis of the results using some of the recently suggested procedures [13,14].

2. Experimental

Commercial alumina powder (Reynolds, USA, purity 99.8%) was treated with analytical reagent (AR) grade magnesium nitrate and was calcined and ground to obtain a powder mix of Al_2O_3 with MgO (0.5 wt.%) additive. This powder mix and Ag_2O powder (Emark India Ltd., purity 98%) were used as the starting materials for the preparation of a series of alumina–silver composites. The chronological steps to prepare these composites are shown in the flow diagram, Fig. 1. Different weight proportions (5, 10 and 15 wt.%) of silver oxide were added to the alumina (with MgO additive) powder to make three different types of alumina–silver composites with varying silver content. Methanol was added to the powder blend to make slurry, which was milled for 8 h using an alumina pot with alumina balls in a laboratory planetary mill. After drying, the resultant powder was crushed in an agate-pestle mortar; during this process polyvinyl alcohol (PVA) solution was added as binder. The agglomeration was then sieved (ASTM No.80) prior to compaction.

The mixed powders were compacted uniaxially at a pressure of 85 MPa to produce square shaped (16×16) pellets of 8 mm thickness. The PVA binder was burnt off by heating the green compacts at 500°C for 5 h. These were then presintered at 1100°C for 2 h followed by final sintering at 1550°C for 2 h using a uniform heating and cooling rate of $\leq 5^\circ\text{C}/\text{min}$. The final sintering was carried out in a programmable electric furnace (UAF-17/12E, Lenton Furnace, UK) under

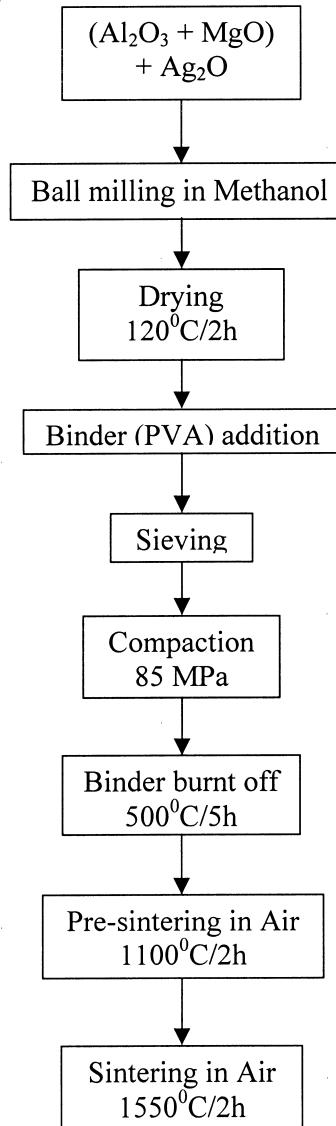


Fig. 1. Flow chart for fabrication of silver toughened alumina composites.

normal atmospheric condition. A series of monolithic alumina specimens with MgO additive were also made following the identical route but using final sintering temperature of 1600°C for 2 h duration.

The sintered pellets were lightly abraded to clear off the unwanted loose particles prior to density measurements. The bulk density, open porosity and relative density were measured employing the boiling water method [17] using Archimedes' principle. The sintered pellets were ground (using 325-grit diamond wheel) to make all the six faces smooth, flat and orthogonal to each other. These specimens were then subjected to standard metallographic polishing using different grades of silicon carbide papers followed by polishing using 3,

1 and 0.25 μm diamond pastes. Phase identification in these samples was made by X-ray diffraction analysis using a Philips made X-ray diffractometer interfaced with a computer. The volume fraction of the silver particles in the different composites was determined by standard point counting method [18]. The spacing between the metallic particles were estimated following an earlier report [19]. The grain size of the matrix was measured by linear intercept method [20] from photographs of fractured surfaces of the specimens taken using a scanning electron microscope (Model 5800, Jeol, Japan).

The hardness values of the prepared composites were measured by the Knoop indentation technique with a microhardness tester (LECO, DM400, Japan). For each measurement at least 10 readings were taken for estimating the average value. These measurements were carried out at loads of 0.49, 0.98, 1.96, 2.94 and 4.9 N using fixed indentation time of 10 s. A series of Vickers hardness tests were also carried out using different loads in the range 49–294 N.

3. Results and discussion

The material design in this investigation has been made to examine varied combinations of physical and mechanical properties vis-a-vis microstructural features of alumina–silver composites containing silver volume fraction in the range of 1–5%. The results related to the nature of the composites, their microstructures and their hardness property are discussed in separate subsections.

3.1. Nature of the composites

Three alumina–silver composites and a monolithic alumina have been considered in this investigation. The amounts of silver oxide added to fabricate the composites were 5, 10 and 15 wt.% and the corresponding materials are referred as Ag-5, Ag-10 and Ag-15 in the subsequent discussion. The selected amounts of silver oxide refer to theoretical silver contents of 1.82, 3.76 and 5.8 percentage volume fraction in the matrix. These selections are based on the available information that hardness of these composites monotonically decreases with increase in the volume fraction of silver, whereas the fracture toughness and flexural strength do not improve significantly with addition of silver beyond 5–6 vol.% [9,11]. The use of MgO additive in alumina has been made with the consideration that it may prevent abnormal grain growth [21], though it is known that silver also assists in inhibiting grain growth [9,11]. During presintering and sintering stages, the decomposition of Ag_2O takes place at $\sim 425^\circ\text{C}$ [9], melting of Ag occurs at 962°C [22] and then some evaporation of Ag occurs at and above 1000°C ; the evaporation rate increases

with the increase in temperature. The vapour pressure of Ag is found reported as 1, 10 and 40 mm of Hg at 1357 , 1575 and 1743°C respectively [22]. The process of evaporation of Ag from alumina–silver system occurs primarily from the surface of the compacted pellets. These result in almost a silver free surface ($\approx 375\ \mu\text{m}$ thick) with a core which is rich in silver. A typical hybrid macrostructure of a pellet is shown in Fig. 2. The relative density of Ag-5, Ag-10 and Ag-15 were found to be 96.19, 97.96 and 94.20% compared to that of Ag-0 as 98.06%. The relatively higher density of Ag-10 specimens compared to those of Ag-5 and Ag-15 specimens are considered to emerge from uncertain minor fluctuations in the processing parameters during the preparation of these composites.

3.2. Microstructure of the composites

The aims involved in the microstructural analysis were to generate information about the grain size of the matrix and the size and inter-spacing of the metallic silver particles dispersed in the matrix. The revelation of the grain size of the alumina matrix was done on the fractured surfaces of the prepared materials using SEM. The average size and average interspacing of silver particles were, however, carried out by light microscopy, because of the large differences in the refractive indices of the matrix and the metallic phase. Typical matrix grain size and distribution of silver particles are illustrated in Figs. 3 and 4 respectively.

The matrix grain size of all the developed composites, as estimated by linear intercept method, can be designated to have an average value of $1.4 \pm 0.2\ \mu\text{m}$. This is in contrast to the reported values of 5.2 – $6.8\ \mu\text{m}$ [9] and 3 – $11\ \mu\text{m}$ [11] for different composition of the alumina–silver composites prepared using different sintering temperatures in some earlier investigations. The obtained smaller grain size in this investigation is attributed to the employment of lower sintering temperature, and use of lower initial alumina particle size ($0.34\ \mu\text{m}$) and MgO

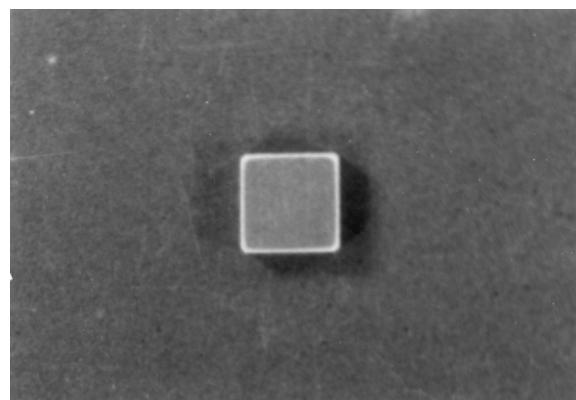


Fig. 2. Macrostructure of an Ag-15 specimen showing silver depleted rim and silver rich core.

additive. An examination of a few earlier reports on grain size of alumina reveals that this could be 1.48 μm [23] and 1.7–2.0 μm [24], and the present results of grain size measurement appear to be in good correspondence with these reported values.

The volume fraction of Ag, obtained by point counting method, were found to be 1.6, 3.38 and 5.01% in Ag-5, Ag-10 and Ag-15 specimens respectively. The experimentally obtained volume fraction values of Ag are approximately 10–15% lower than the values obtained by theoretical calculations. The observed lower values of Ag from experimental measurements primarily arise from the loss of silver during sintering; a rough estimate indicates similar equivalent amount of weight loss from the compacted pellets after presintering. The mean size of the Ag particles were found to increase with increased addition of Ag to the composites. On the other hand, the estimated mean inter-particle spacing were found to decrease. The variations of these microstructural features in the prepared composites are portrayed as a bar diagram in Fig. 5. The distribution of Ag particles in the microstructures may better be

referred as bimodal because 95% of the particles centers around the mean size whereas the rest are larger and range between ~ 5 and 10 μm . It may be mentioned at this stage that even though the amount of Ag was ≤ 5 vol.% in the prepared composites, its presence could be detected by X-ray diffraction analysis as shown in Fig. 6.

3.3. Hardness

A series of hardness measurements were attempted on the developed alumina–silver composites using indentation loads between 49 and 294 N with the help of a Vickers hardness tester. It was noticed that indentations taken at these loads are associated with crushed corners or edges with cracks emanated from the corners. Thus any attempt to estimate Vickers hardness values (H_V) at these loads would yield invalid hardness results on these investigated composites. To overcome this difficulty, Knoop indentations were made at different loads between 0.498 and 4.98 N and the indentation diagonals

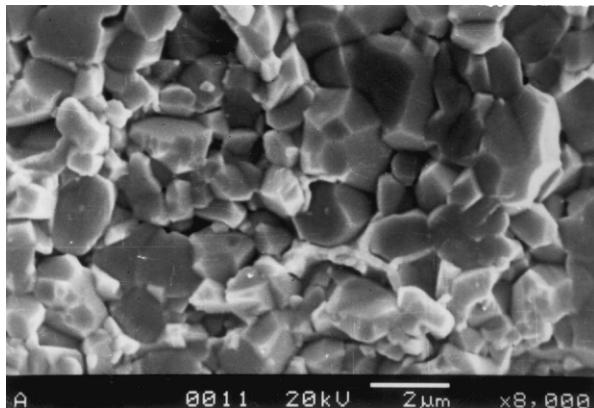


Fig. 3. Typical fractograph of an Ag-15 composite used for grain size measurement.

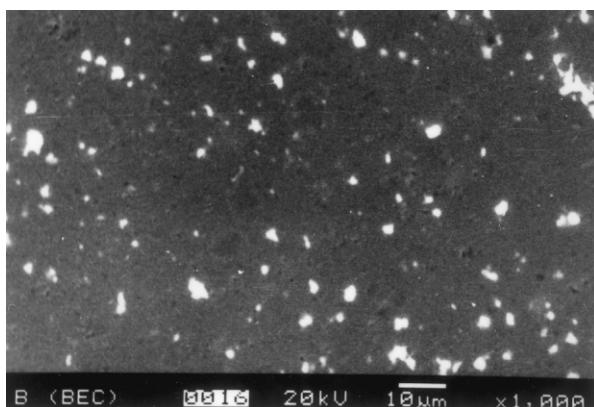


Fig. 4. Typical uniform distribution of silver particles in the central region of an Ag-15 specimen.

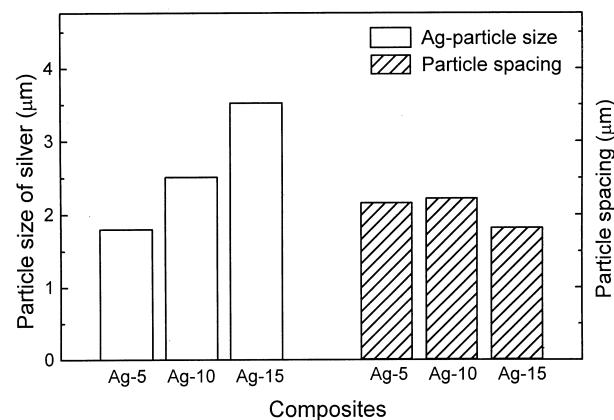


Fig. 5. Average particle size and particle spacing in the developed alumina–silver composites.

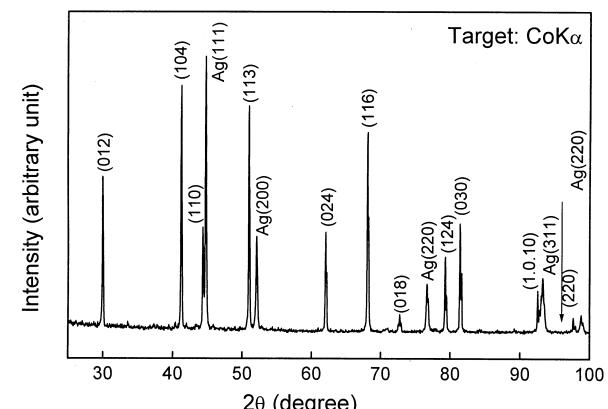


Fig. 6. Typical X-ray diffraction spectrum of an Ag-15 composite exhibiting both Ag and α - Al_2O_3 peaks (phases: α - Al_2O_3 - no coding, silver- Ag).

were measured. Unlike the Vickers hardnesses, the Knoop indentations could be revealed distinctly on the video screen of the microhardness tester and additionally these indentations were found to be free from crushed edges or corners. At the outset average Knoop hardness values (H_K) were determined at different loads from the measurement of major diagonal lengths. These estimations are shown in Fig. 7. The load dependence of hardness or indentation size effect in all specimens Ag-0, Ag-5, Ag-10 and Ag-15 is quite pronounced and the nature of decrease of hardness with increasing load is of the same form in all the materials. These results uniquely infer that it is inappropriate to assign a unique hardness value, estimated by conventional procedure, to any of these materials without indicating the indentation load. This inference can be considered to be of generalized nature for similar brittle materials. As a consequence any comparison of hardness values of the developed materials with the earlier reported data is difficult unless such measurements are carried out at identical load and for identical indentation duration.

The indentation size effect in ceramics and glasses has been analysed using different approaches by earlier investigators [13–16]. The load dependence of hardness has been considered by Li et al. [13] and Ray and Dutta [14] to originate from the fact that the measured diagonal of an indentation at a particular load is an apparent value, which remains associated with an uncertain amount of relaxation. The extent of relaxation in an indentation diagonal (d_e) occurs due to several possibilities such as crack formation, dislocation activity and elastic recovery at the tip of the indentation [13,14]. It is thus necessary to estimate the intrinsic hardness of a material by accounting the above phenomena.

Li et al. [13] have suggested that an estimation of true hardness can be made by measuring Knoop hardness at different loads and by considering the following relations:

$$d = d_o + d_e \quad (1)$$

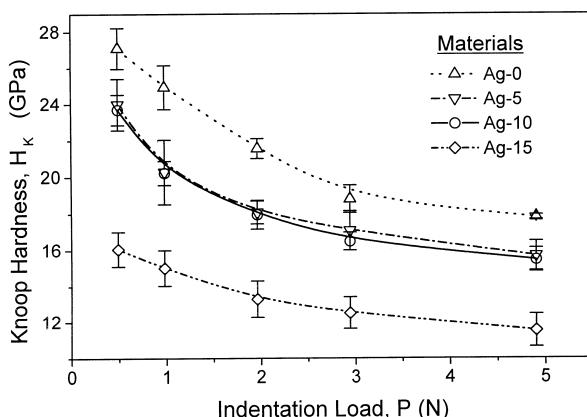


Fig. 7. Influence of load on microhardness for different materials.

$$H_o = 14229P/(d_o)^2 \quad (2)$$

$$H_k = 14229P/d^2 \quad (3)$$

$$H_k = H_o(1 + d_e/d)^2 \quad (4)$$

$$d = (14229/H_o)^{1/2}P^{1/2} - d_e \quad (5)$$

where d and d_o are measured and true diagonal lengths, d_e is the amount of relaxation on diagonal lengths, and H_o and H_k are true and apparent hardness values.

Eq. (5) indicates that measured indentation diagonals (d) should bear linear relationship with the square root of the indentation load and the slope of such a curve would yield the value of true hardness (H_o). The load dependence of indentation diagonals for Ag-0, Ag-5, Ag-10 and Ag-15 specimens was reanalyzed as d vs. $P^{1/2}$ plots in Fig. 8. It was noted that such plots are linear in nature with the estimated linear regression coefficients (LRC) always better than 99.9%. This observation permits one to calculate the true hardness of these materials from the computed values of the slopes as shown in Fig. 8 together with the associated LRC. The true hardness values of the investigated samples vis-a-vis H_k at 4.98 N load are illustrated as a function of Ag content in Fig. 9. These results indicate that true hardness of the material in general is lower than that of the conventionally estimated ones. This observation is in agreement with similar experimental results in silicon carbide composites [13] and in soda-lime-silica glass [14]. The computations of H_o values for the investigated materials also indicated that the magnitude of d_e to be 5.2 μm for alumina and 6.1–6.4 μm for alumina-silver composites. These estimated magnitudes of d_e infer that the amount of relaxation of diagonal length is significant with respect to the measured diagonals at low indentation loads and hence the indentation size effect is found to be pronounced for the low load range.

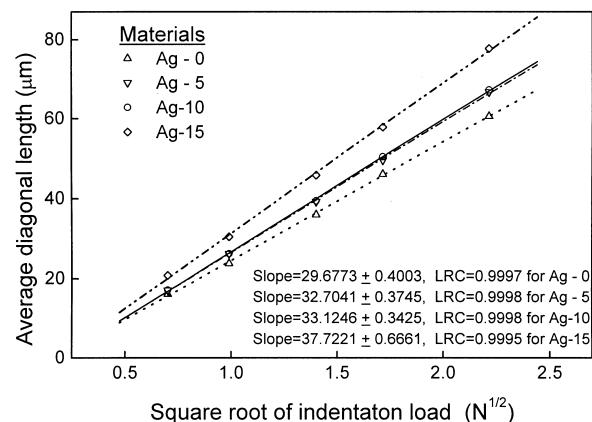


Fig. 8. Plots of diagonals of Knoop indentation vs. square root of indentation loads for the developed materials.

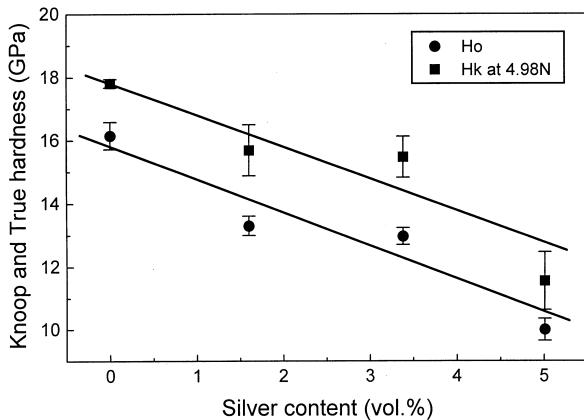


Fig. 9. True and apparent Knoop hardness values of the developed materials.

Quinn and Quinn [15] have recently examined the variation of Vickers hardness with indentation load for a variety of ceramic materials. These investigators observed that such hardness-load curves exhibit distinct transition to a plateau of the constant hardness level and concluded that the transition in such curves correspond to the intrinsic hardness value of the material. These investigators [15] have proposed an energy balance model for the Vickers indentation process. The model considers that the external work applied by the indenter is consumed in deformation and fracture process in the material. This model is compatible to a modified Meyer's law type equation

$$Pd = a_1 d^2 + a_2 d^3 \quad (6)$$

The left-hand side of Eq. (6) may be related to external work done by the indenter, the first term on the right hand side of the equation represents energy expended in the material in the process of creating new surface area whereas the second term corresponds to the volume energy. The latter includes the material deformation resulting from the indentation and may be expressed in terms of a specific strain energy times the deformation volume. In the present investigation the Knoop hardness values have been estimated at a relatively larger intervals of load and the type of transition observed by Quinn and Quinn [15] has not been revealed. Hence no attempt has been directed to obtain the plateau hardness value. Additionally Li et al. [13] have observed that hardness-load curves exhibit the distinct transition to a plateau, as mentioned by Quinn and Quinn [15], only for Vickers indentation and found a monotonic decrease in H_K at higher loads for Knoop indentation. It is thus uncertain whether such distinct transition point to constant hardness is characteristics of H_K -load curves or not.

Li and Bradt [16] have also found the nature of load dependence of Knoop hardness similar to the results

obtained in the present investigation. But instead of incorporating the concept of relaxed diagonal, these investigators [16] indicate that the load-indentation diagonal relationship in Knoop hardness testing may be better described by a normalized Meyer's law.

$$P = \frac{2P_c}{n} \left(\frac{d}{d_0^*} \right)^n \quad (7)$$

where P_c is a critical test load indicative of the region where hardness is independent of the indentation test load and d_0^* is a characteristic indentation dimension, below which the indentation size effect is significant. These investigators [16] have suggested that d_0 value calculated from H_o may not be completely free from the indentation size effect and have proposed the multi-parameter approach of critical load and characteristic indentation dimension to describe the load-indentation curve. However, the force fitting of Eqs. (7) or (5) to experimentally obtain load-diagonal values in Knoop hardness testing needs to be carefully examined for load dependence of Knoop hardness for several materials before arriving at any definite inference with respect to the comparative merits of these equations.

The Knoop hardness values of Ag-0 samples (Fig. 7) lie in the range of 27–18 GPa for indentation loads of 0.498–4.98 N respectively. The lower bound of these estimated values is similar to the reported hardness value of alumina. Kim [25] has reported the hardness of alumina to be 17–19 GPa. However, such comparisons are inappropriate because the materials considered in the different investigations can lead to different hardness values, simply depending on their varied sintered density, grain size, impurity content etc. But apparently the compatibility of the measured hardness values of the prepared Ag-0 samples at 4.98 N load with those of the reported ones provide a guideline that such measurements on alumina–silver composites can be considered to be reliable in nature. A comparison of the hardness values of the alumina–silver composites with those of Ag-0 sample infers that hardness of the former materials decreases with increase in their silver content. This observation is in agreement with the nature of the results reported by Wang et al. [9] and Chou and Tuan [11] on this system. The earlier investigators [9,11], however, have examined such property for alumina–silver composites containing much higher volume fractions (6.6–12.4% [9]) of the silver phase. The results of hardness measurements thus lead to the conclusions that: (a) hardness of alumina or alumina based composites should be examined by appropriate consideration of their load dependence and (b) the hardness of alumina–silver composites decreases with increased volume fraction of silver in these materials.

4. Conclusions

Pressureless sintering at 1550°C can be used to produce alumina–silver composites with high relative density and clean interface between the matrix and the reinforced metal particles. The specimens exhibit a gradient microstructure with a silver rich core and a silver depleted rim. The particle size of silver in these composites increases with increased addition of silver oxide, attended with decreased inter-spacing of the particles in the domain of this investigation.

The hardness values of the core region of these composites are found to be sensitive functions of indentation load. An analysis has been made to estimate the true hardness of alumina–silver composites for the first time. The true hardness of these composites decreases with increase in silver content.

References

- [1] M.S. Newkirk, H.D. Lesser, D.R. White, C.R. Kennedy, A.W. Urquhart, T.D. Clarr, Preparation of Lanxide ceramic matrix composites: matrix formation by the directed oxidation of molten metals, *Ceram. Eng. Sci. Proc.* (1987) 879–885.
- [2] X. Gu, R.J. Hand, The production of reinforced aluminium/alumina bodies by directed metal oxidation, *J. Eur. Ceram. Soc.* 15 (1995) 823–831.
- [3] X. Zhang, G. Lu, M.J. Hoffmann, R. Metselaar, Properties and interface structures of Ni and Ni–Ti alloy toughened Al_2O_3 ceramic composites, *J. Eur. Ceram. Soc.* 15 (1995) 225–232.
- [4] X. Sun, J.A. Yeomans, Microstructure and fracture toughness of nickel particle toughened alumina matrix composites, *J. Mater. Sci.* 31 (1996) 875–880.
- [5] R.Z. Chen, W.H. Tuan, Pressureless sintering of Al_2O_3 /Ni nanocomposites, *J. Eur. Ceram. Soc.* 19 (1999) 463–468.
- [6] P.A. Trusty, J.A. Yeomans, The toughening of alumina with iron: effects of iron distribution on fracture toughness, *J. Eur. Ceram. Soc.* 17 (1997) 495–504.
- [7] M. Nawa, T. Sekino, K. Niihara, Fabrication and mechanical behaviour of Al_2O_3 /Mo composites, *J. Mater. Sci.* 29 (1994) 3185–3192.
- [8] Y. Waku, M. Suzuki, Y. Oda, Y. Kohtoku, Influence of particle size and volume percent of flaky Mo particles on the mechanical properties of Al_2O_3 /Mo composites, *Metall. Mater. Trans. A* 27A (1996) 3307–3317.
- [9] J. Wang, C.B. Ponton, P.M. Marquis, Silver-toughened alumina ceramic, *Brit. Ceram. Trans.* 92 (1993) 67–74.
- [10] J. Wang, C.B. Ponton, P.M. Marquis, The microstructure of pressureless sintered silver-toughened alumina: an in situ TEM study, *Mater. Sci. Eng. A* 161 (1993) 119–126.
- [11] W.B. Chou, W.H. Tuan, Toughening and strengthening of alumina with silver inclusions, *J. Eur. Ceram. Soc.* 15 (1995) 291–295.
- [12] W.H. Tuan, W.B. Chou, The corrosion behavior of Al_2O_3 toughened by Ag particles, *J. Eur. Ceram. Soc.* 16 (1996) 583–586.
- [13] Z. Li, A. Ghosh, A.S. Kobayashi, R.C. Bradt, Indentation fracture toughness of sintered silicon carbide in Palmqvist crack regime, *J. Am. Ceram. Soc.* 72 (1989) 904–911.
- [14] K.K. Ray, A.K. Dutta, Comparative study on indentation fracture toughness evaluations of a soda-lime–silica glass, *Brit. Ceram. Trans.* 98 (1999) 165–171.
- [15] H. Li, R.C. Bradt, Knoop microhardness anisotropy of single-crystal LaB_6 , *Mater. Sci. Eng. A* 142 (1991) 51–61.
- [16] J.B. Quinn, G.D. Quinn, Indentation brittleness of ceramics: a fresh approach, *J. Mater. Sci.* 32 (1997) 4331–4346.
- [17] W.D. Kingery, H.K. Bowen, D.R. Uhlmann, *Introduction to Ceramics*, 2nd Edition, John Wiley & Sons, New York, 1976, p. 531.
- [18] ASTM Standard E562-89, Standard test method for determining volume fraction by systematic manual point count, ASTM Pub., Pennsylvania, USA, 1993, 03.01, pp. 612–617.
- [19] K.K. Ray, D. Mondal, Some aspects of deformation behaviour of coarse multiphase metallic materials, *Metall. Trans. A* 23A (1992) 3309–3315.
- [20] ASTM Standard E112-88, Standard test methods for determining average grain size, ASTM Pub., Pennsylvania, USA, 1993, 03.01, pp. 297–322.
- [21] S.I. Bae, S. Baik, Critical concentration of MgO for the prevention of abnormal grain growth in alumina, *J. Am. Ceram. Soc.* 77 (1994) 2499–2504.
- [22] D.R. Lide, (Ed.), *CRC Hand Book of Chemistry and Physics*, 72nd Edition, CRC Press, Boston, USA, 1991, p. 4–95, 6–67.
- [23] H. Erkalfa, Z. Misirli, C. Toy, T. Baykara, The densification and microstructural development of Al_2O_3 with manganese oxide addition, *J. Eur. Ceram. Soc.* 15 (1995) 165–171.
- [24] R.W. Davidge, R.C. Piller, A. Briggs, I.E. Denton, R.J. Brock, U. Eisele, H. Hodgson, A.J. Jones, T. Dupin, M.P. Titeux, C.A. Elyard, G. Partidge, D.R. Cooper, Advanced alumina products from high purity alumina powders, in: H. Nosbusch, I.V. Mitchell (Eds.), *Commission of the European Communities, Technical Ceramics*, Elsevier Applied Science, London and New York, 1998, pp. 163–173.
- [25] S. Kim, Material properties of ceramic cutting tools, *Key Eng. Mater.* 96 (1994) 33–80.